



# Exploring the potential of graphene oxide frameworks as anode materials for Na-ion batteries applications: a density functional theory study

F. Peymanirad<sup>1</sup> · R. Majidi<sup>2</sup> · S. Izadi Vishkayi<sup>3</sup> · H. Rahimpour Soleimani<sup>1</sup>

Received: 2 January 2024 / Accepted: 19 March 2024 / Published online: 17 April 2024  
© The Author(s), under exclusive licence to Springer-Verlag GmbH Germany, part of Springer Nature 2024

## Abstract

This study explores the potential applications of graphene oxide frameworks (GOFs) in Na-ion batteries using density functional theory calculations. The GOF's graphene layers are linked by benzenediboronic acid pillars. Ab-initio molecular dynamics simulations demonstrate the thermal stability of the structures. The study calculates adsorption and barrier energy, storage capacity, and open-circuit voltage. The results predict the high mobility of Na in GOF due to the low energy barrier. The layered structure of GOF enables the intercalation of Na-ions. GOF has a Na storage capacity of 947 mAh/g in the form of Na<sub>21</sub>C<sub>36</sub>, which is higher than the reported values for graphite and some other two-dimensional carbon-based materials. The transition from semiconductor to metal, which is an essential condition for the diffusion of ions within the anode material, occurs after Na adsorption. Therefore, GOFs are a promising anode material with high efficiency for Na-ion batteries.

**Keywords** Na-ion battery · Graphene oxide frameworks · 1,4-Phenyldiboronic acid · Anode material · Theoretical storage capacity · Density functional theory

## 1 Introduction

The creation of new green and clean energy sources is required because fossil fuel resources are non-renewable and harmful to the environment. Rechargeable ion batteries play a crucial role in reducing our carbon footprint [1, 2]. Li-ion batteries are rechargeable batteries that have received much attention in recent years, especially when combined with carbon-based materials. Graphite is widely used as an anode material in Li-ion batteries due to its low cost, low toxicity, high abundance, electrochemical characteristics, and renewable potential [1, 3, 4]. Its layered structure allows the intercalation of Li-ions, resulting in an impressive

theoretical capacity of 372 mAh/g in the form of LiC<sub>6</sub> [4]. In addition to graphite, there are two-dimensional (2D) carbon-based materials with capacities greater than 372 mAh/g. For instance, graphene has a specific capacity of 744 mAh/g if Li can be absorbed on both sides of the sheet up to the chemical formula Li<sub>2</sub>C<sub>6</sub>. This specific capacity is twice higher than that of graphite [5, 6]. Further, 2D carbon-based materials such as T-graphene, graphyne, and graphdiyne sheets delivered capacity much greater than the corresponding values of graphite and graphene [7–10]. Thus, these nanomaterials can be a promising anode for high-capacity Li-ion batteries.

In addition to Li-ion batteries, Na-ion batteries have received a lot of attention. On the one hand, this interest is owing to the low cost, abundance, and safety of Na, and on the other hand, it is due to the lack of Li resources and high water consumption in Li production [11]. Despite the growing research in Na-ion batteries, the implementation of these batteries has been practically hindered by the fact that Na-ion batteries have a lower voltage (2.5 V) than Li-ion batteries (3.7 V) [12]. Also, Li-ion is smaller than Na-ion in terms of mass and atomic radius [13]. Thus, Na-ions can hardly intercalate into layers of graphite. Various reports have shown that the distance between the carbon layers must be greater than 0.37 nm to achieve the insertion of a Na-ion

✉ R. Majidi  
royamajidi@gmail.com

<sup>1</sup> Computational Nanophysics Laboratory (CNL), Department of Physics, University of Guilan, P. O. Box 41335-1914, Rasht, Iran

<sup>2</sup> Department of Physics, Shahid Rajaei Teacher Training University, Lavizan, 16788-15811, Tehran, Iran

<sup>3</sup> School of Physics, Institute for Research in Fundamental Science (IPM), P.O. Box 19395-5531, Tehran, Iran

into the carbon layers [14]. The graphite only has a layer spacing of 0.34 nm, which is not enough for Na-ions. Thus, without modification, the common graphite is not efficient for Na-ion anodes due to its extremely low capacity of 35 mAh/g in the form of  $\text{NaC}_{64}$  [15].

One approach to enhance the Na-ion storage capacity is finding porous materials with a large space between their layers. There may be space for Na adsorption in graphyne and graphdiyne, with rings that are larger than the hexagonal rings of graphene [16]. It can be seen that the Na adsorption on single and bulk layers of graphdiyne causes a theoretical capacity of 497 and 316 mAh/g, respectively [17]. Twin graphene also has a theoretical capacitance of 496 mAh/g close to that of graphdiyne [9]. For pentagraphyne, a high theoretical capacitance of 680 mAh/g for Na-ions is determined [9, 18]. Recently, T-graphene, twin T-graphene, and  $T_{4,4,4}$ -graphyne with Na theoretical capacities of 2357, 2231, and 1984 mAh/g are reported [7, 19, 20]. As an anode in Na-ion batteries, the theoretical storage capacity of these sheets is meaningfully more than graphene and graphdiyne.

Increasing the distance between layers of graphite is an effective method to store an appropriate number of Na-ions [21]. For instance, a two-step oxidation–reduction process is used to create an expanded graphite [22]. This modified graphite oxide (GO) exhibits an interlayer distance of 0.43 nm. As a result, the expanded graphite could achieve a high specific capacity for Na [22]. The Na-ion storage capacity of GO is also investigated. The results demonstrated that Na-ions are adsorbed close to the epoxide groups with favorable energies. Thus, Na-ion batteries may use the suggested sheets as anode candidates for future Na-ion batteries with a high rate of specific capacity as a result of epoxide groups [23]. However, not all carbon atoms and available space are accessible for absorption or storage of gas because GO typically contains various functional groups, including hydroxide, epoxide, carbonyl, and carboxyl groups [24].

According to recent studies, the interlayer distance has increased to approximately 1.1 nm in open GO structures made of pillared GO layers [23–26]. These new materials, known as graphene-oxide frameworks (GOFs), have been reported to form as a result of the solvothermal reaction of GO with benzene-1,4-diboronic acid, 1,4-phenylenediboronic [26]. Between graphene layers, benzenediboronic acid pillars aid in separating the layers and offer adequate adsorption space. It has been found that these synthesized GOFs have thermal stability up to 550 K, and they are highly tunable materials with electronic properties ranging from metals to semiconductors [27]. The GOFs may have significant applications in gas sensing, storage, sorption, and separation, as well as energy storage [25, 28–30].

As developing materials for batteries is a hopeful method to improve their performance meaningfully, the potential applications of GOF with benzenediboronic acid pillars as an anode in

Na-ion batteries are investigated by density functional theory calculations (DFT) in the present study.

## 2 Computational details

The OpenMX3.9 package is used to perform the DFT calculations [31]. The Perdew–Burke–Ernzerhof (PBE) function and the generalized gradient approximation (GGA) are employed for energy exchange and correlation functional [32]. The Van der Waals (vdW) effect is taken into account using the DFT-D3 method [33, 34]. The cutoff energy of 400 Ry is considered during the calculations. A vacuum layer of about 15 Å along the direction normal to the graphene sheets is assumed to avoid the interaction between repeated images. The simulation cells are subjected to the periodic boundary conditions along all directions. The configurations are optimized until the force component on every atom is less than 0.005 eV/Å. To understand the electronic properties, the density of states (DOS) and the electronic band structures are calculated. Ab initio molecular dynamics (AIMD) simulations are performed to look at the thermodynamical characteristics of the structures. The time step is 1 fs, and all structures are heated to a temperature of 300 K for up to 10 ps. A Nose–Hoover thermostat is employed to control the temperature. The nudged elastic band approach is used to investigate the diffusion pathways and corresponding energy barriers of a single Na atom inside GOF [35].

## 3 Results and discussion

The optimized structure of GOF is presented in Fig. 1. A graphene sheet can be seen from the top. It is obvious from the side that two parallel layers of graphene are linked by benzenediboronic acid. One benzenediboronic molecule for every 18 carbon atoms of each graphene layer is considered perpendicular to the graphene layers as a pillar. The interlayer distance between graphene in GOF is found to be between 10.2 and 11.5 Å, which was reported in a previous study to be close to 11.7 Å [28].

Many different sites are assumed to identify the most stable site for the adsorption of Na. Some sites with high symmetry are shown in Fig. 1. The adsorption energy,  $E_{ads}$ , of Na atom on GOF is estimated according to the following equation to find the best adsorption site in terms of energy:

$$E_{ads} = \frac{E_{GOF+Na} - (E_{GOF} + n_{Na}E_{Na})}{n_{Na}} \quad (1)$$

here,  $E_{GOF+Na}$  and  $E_{GOF}$  are the total energy of GOF with and without Na, respectively.  $E_{Na}$  denotes the energy of a single Na atom in bulk, and  $n_{Na}$  is the number of adsorbed Na atoms. Based on this equation, a negative value indicates an

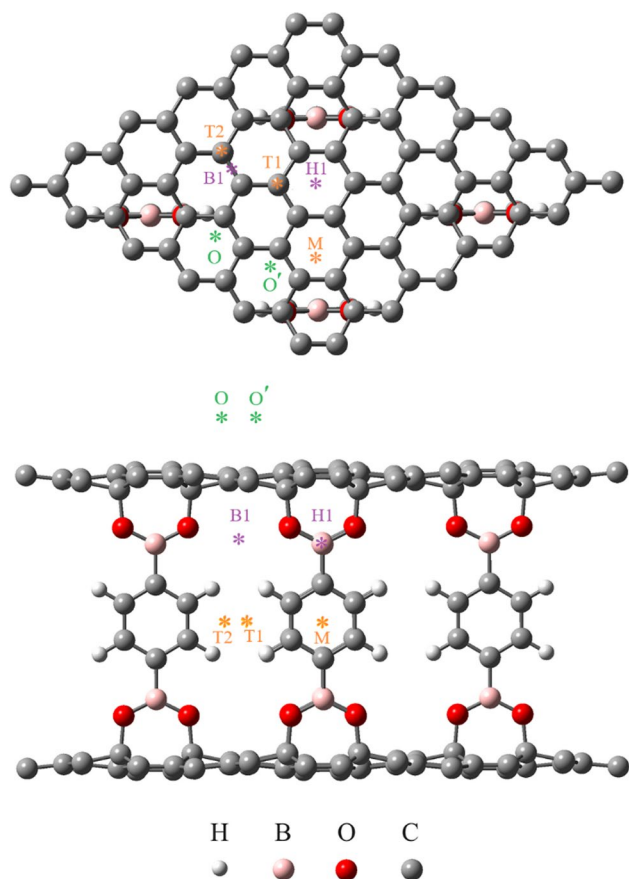


**Fig. 1** Atomic structure of GOF from top and side views. (The sites for Na adsorption are shown by \*)

energetically stable configuration and more negative energy indicates a more favorable structure. The comparison of the energy values shows that in the first step, Na atom prefers to be absorbed in the space between the graphene layers at B1-site. This configuration yields an adsorption energy of  $-2.23$  eV/Na, which is more negative than the adsorption energy of other configurations. The nearest distance between the adsorbed Na atom and C atom of graphene sheets is  $2.6$  Å, and the smallest distance of Na atom from the graphene sheet is  $2.5$  Å. The nearest distance between Na atom and H, O, and B atoms of the acid is  $2.8$ ,  $2.9$ , and  $3.8$  Å, respectively.

The second preferred adsorption site is H1-site. The adsorption energy for Na at this site is found to be  $-1.75$  eV. At H1-site, the smallest distance between the C and Na atoms is  $2.9$  Å and its distance from the graphene sheet is  $2.6$  Å. The M-site is found to be the third most favorable adsorption site. After full optimizations, Na atom is placed exactly in the middle of the graphene layers. Other adsorption sites with their corresponding adsorption energies are presented in Table 1. It is important to note that the magnitude of the adsorption energy must be between  $-1.13$  and  $-3.0$  eV to

**Table 1** Adsorption site, closest distance between C and Na atoms,  $d_{\text{Na-C}}$ , smallest distance of Na atom from the graphene sheet,  $d_{\text{Na-sheet}}$ , and adsorption energy,  $E_{\text{ads}}$ . (The sites for Na adsorption are shown in Fig. 1)

Adsorption site	$d_{\text{Na-C}}$ (Å)	$d_{\text{Na-sheet}}$ (Å)	$E_{\text{ads}}$ (eV)
B1	2.6	2.5	$-2.23$
H1	2.9	2.6	$-1.75$
M	5.8	5.7	$-1.13$
T1	5.6	5.6	$-0.96$
T2	5.5	5.5	$-0.87$
O, O'	2.6	2.5	$-0.69$

allow the adsorption and desorption of a suitable material as an anode in ion batteries [36]. The values of adsorption energy for Na adsorption inside GOF indicate that GOF is a proper material to use in Na-ion batteries. The magnitude of the adsorption energy is calculated by incorporating the vdW corrections. Our calculations indicate that the vdW effect increases the magnitude of the adsorption energy by a very small amount (about  $0.02$  eV) compared to the case without vdW corrections.

The mobility of Na atoms is an important factor that plays an important role in the performance of electrode materials for rechargeable ion batteries. The rapid charging or discharging rates of Na-ion battery are confirmed by the lower ionic diffusion barrier. Thus, it is crucial to take into account the diffusion pathway of Na ions on GOF. It is necessary to consider the diffusion path of a single Na atom on GOF. The energy barriers corresponding to paths 1 and 2 are presented in Fig. 2. Here, the barriers are not considerable and can be easily overcome. The small barriers allow Na-ions to move quickly. According to our findings, GOF has diffusion energy barriers close to the sheets such as T-graphene, graphyne, and graphdiyne (around  $0.4$  eV) [7, 8, 16, 37, 38].

The maximum number of adsorbed ions is another factor that has a significant impact on the ion battery's efficiency. The Na atoms are located on the stable sites, and their concentration is gradually increased to assess the maximum Na storage capacity of GOF. The number of adsorbed Na atoms could be increased as long as the adsorption energy is within the proper range (between  $-1.13$  to  $-3.0$  eV) [36, 39], or Na atoms could form clusters.

The B1-sites are entirely occupied by Na atoms in the first step. On each graphene layer of GOF, there are two B1-sites. As a result, on these sites, four Na atoms are sandwiched between graphene layers of GOF. The  $\text{Na}_4\text{C}_{36}$  is a structure with adsorption energy of  $-1.44$  eV/Na that results from this Na loading. All H1-sites, the second favorable adsorption site, are filled after B1-sites. There are two H1-sites in GOF, as can be seen. Four Na atoms could have occupied H1-sites on both graphene layers of GOF, resulting in the  $\text{Na}_8\text{C}_{36}$  structure. The adsorption energy of  $\text{Na}_8\text{C}_{36}$  is  $-1.20$  eV/

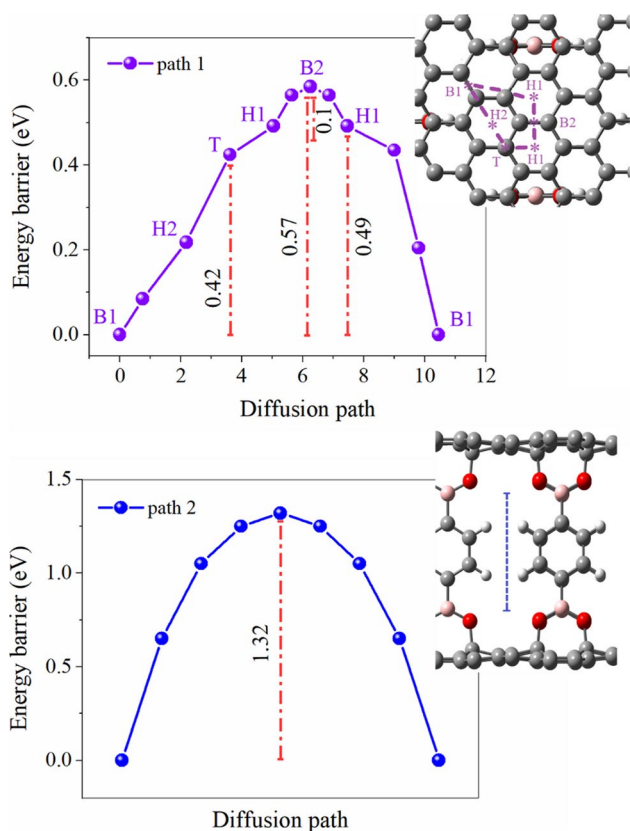


**Fig. 2** The energy profile of Na diffusion on GOF

Na. In the third step, one Na atom is placed at M-site. The adsorption energy of the  $\text{Na}_6\text{C}_{36}$  structure is  $-1.28$  eV/Na. In the following, T1- and T2-sites are occupied. The adsorption energy of the  $\text{Na}_{11}\text{C}_{36}$  and  $\text{Na}_{13}\text{C}_{36}$  structures is  $-1.36$  and  $-1.33$  eV/Na, respectively. The adsorption energy of  $\text{Na}_{13}\text{C}_{36}$  ( $-1.33$  eV/Na) is still higher than the adsorption energy of Na ( $-1.13$  eV/Na [36, 39]). As a result, there might be more Na atoms. It should be noted that in addition to the adsorption energy, the distance between Na atoms is an important factor. The space between two graphene layers is not enough to increase the number of atoms. When 14th Na atoms are added, the distance between Na atoms becomes less than  $2.4 \text{ \AA}$ , and they form bonds with each other. Hence, the next Na atoms are placed outside the inter-space of the structure. It is found that four carbon atoms can be adsorbed without clustering on each graphene layer. The  $\text{Na}_{21}\text{C}_{36}$  structure has an adsorption energy of  $-1.29$  eV/Na. The 22th Na forms bonds with other Na atoms because of their close proximity. Thus, adsorption of 22 Na atom without clustering is not possible. The atomic structure of GOF with 21 Na atoms in the form of  $\text{Na}_{21}\text{C}_{36}$  is shown in Fig. 3. As can be seen, the adsorbed Na atoms form 5 layers. Each Na layer is also illustrated from the top view.

The average adsorption energy,  $E_{\text{avg}}$ , is defined as:

$$E_{\text{avg}} = \frac{E_{(\text{sheet}+\text{Na})_n} - E_{(\text{sheet}+\text{Na})_{n-1}} - xE_{\text{Na}}}{x} \quad (2)$$

in order,  $E_{(\text{sheet}+\text{Na})_n}$  and  $E_{(\text{sheet}+\text{Na})_{n-1}}$  represent the total energy of GOF with  $n$  and  $(n-1)$  layers of adsorbed Na atoms. Here,  $E_{\text{Na}}$  is the energy of a single Na atom, and  $x$  is the number of Na atoms in every layer. In the first step, two layers labeled L1 and L2 in Fig. 3 are formed. These structures are equivalent to  $\text{Na}_4\text{C}_{36}$  and  $\text{Na}_8\text{C}_{36}$ , and their average adsorption energy is  $-1.44$  and  $-0.97$  eV/Na, respectively. The third Na layer (L3) inside GOF is placed in the middle of the graphyne sheets and gives an average adsorption energy of  $-1.53$  eV/atom. After fully occupying the inside of the GOF, the next Na layers are placed on the graphene sheets. The average adsorption energy of the fourth and fifth layers (L4 and L5) is  $-1.23$  eV/Na. The values are still above the cohesive energy of Na ( $-1.13$  eV/Na). However, adding more Na atoms is not possible because they form clusters.

The theoretical capacity,  $C$ , of GOF can be predicted as:

$$C = \frac{n_{\text{Na}}F}{M_{\text{GOF}}} \quad (3)$$

here,  $n_{\text{Na}}$  defines the number of adsorbed Na atoms,  $F$  is the Faraday constant ( $26.8 \text{ Ah/mol}$ ), and  $M_{\text{GOF}}$  represents the mass of GOF material. As shown in Fig. 3, GOF can hold 21 Na atoms per considered cell. As a result, the Na storage capacity of the inner space of GOF is  $586 \text{ mAh/g}$ , while its total Na storage capacity is  $947 \text{ mAh/g}$ . Its storage capacity is more than that of single and bulk layers of graphdiyne ( $497$  and  $316 \text{ mAh/g}$ ), twin graphene ( $496 \text{ mAh/g}$ ), and pentagraphyne ( $680 \text{ mAh/g}$ ) [9, 17, 18]. Thus, GOF could be used as an anode in Na-ion batteries.

The AIMD simulations at room temperature are also used to evaluate the thermal stability of structures. For instance, Fig. 4 shows the changes in the total energy of  $\text{Na}_{21}\text{C}_{36}$  during the simulation. It is evident from this that the total energy fluctuates slightly around a constant value. During the simulations, the atomic structure of the systems is followed. The results indicated that the system exhibits no discernible distortions. Thus, the adsorbed system is suitable for practical Na storage, particularly at room temperature, due to its thermodynamic stability.

The next crucial aspect of the batteries is the evaluation of open-circuit voltage (OCV) for the electrode material. It predicts the Na insertion speed from cathode to anode during the charging process and maximum storage capacity. The OCV is determined by [7, 9],

$$\text{OCV} = \frac{E_{\text{GOF}} + n_{\text{Na}}E_{\text{Na}} - E_{\text{GOF}+\text{Na}}}{n_{\text{Na}}e} \quad (4)$$

where,  $n_{\text{Na}}$  represents the number of adsorbed Na atoms, and  $E_{\text{Na}}$  is the energy of a single Na atom in its bulk crystal.

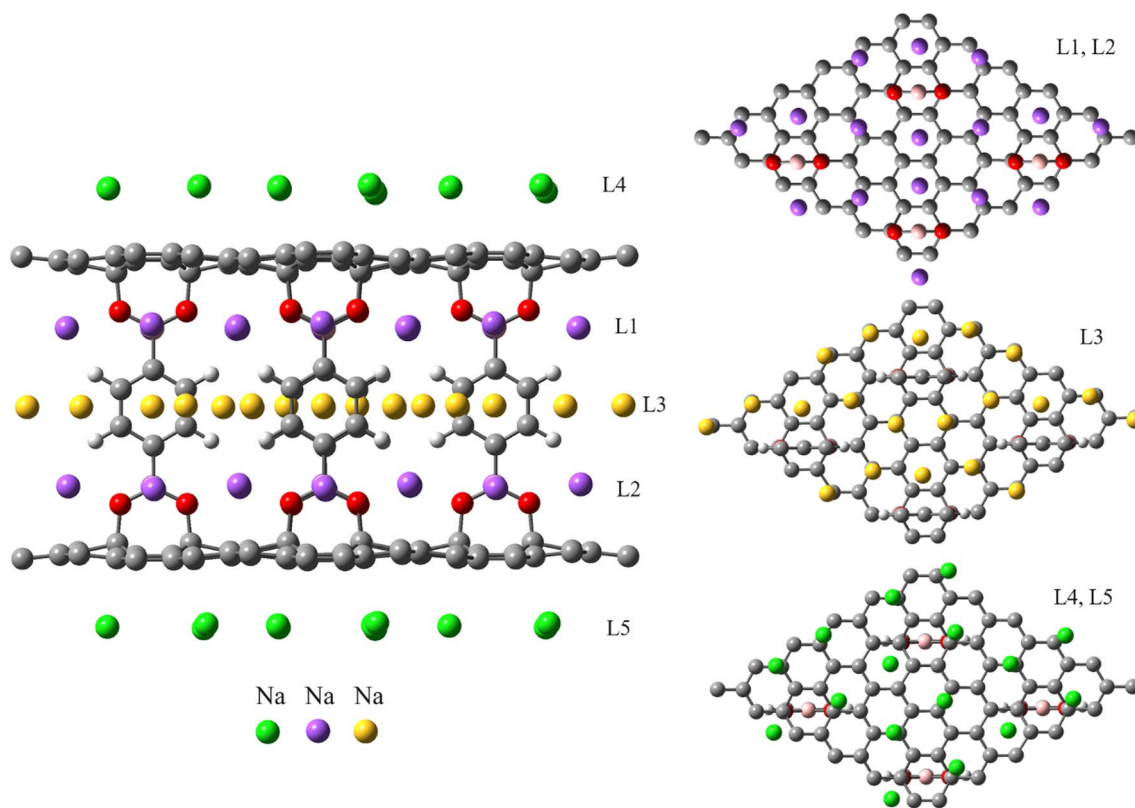


**Fig. 3** Atomic structure of GOF with 21 Na atoms ( $\text{Na}_{21}\text{C}_{36}$ ) from side view. (Each layer of adsorbed Na-atoms is shown from top view)

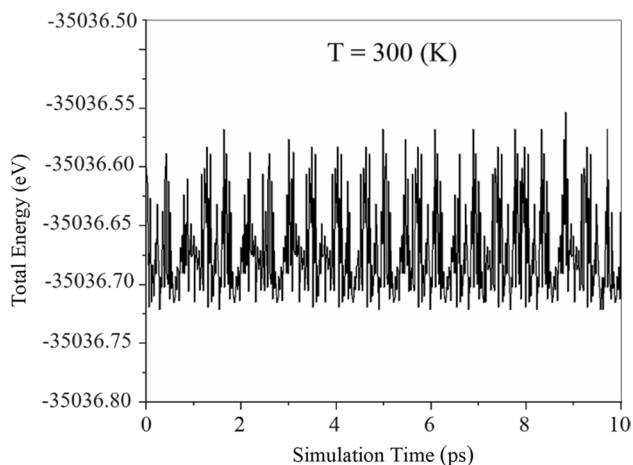


**Fig. 4** Total energy as a function of the simulation time for  $\text{Na}_{21}\text{C}_{36}$  at  $T = 300$  K

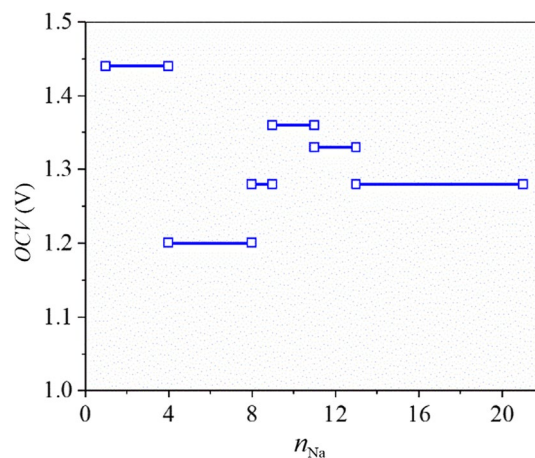


**Fig. 5** Open-circuit voltage,  $OCV$ , as a function of the number of Na atoms adsorbed on GOF,  $n_{\text{Na}}$

The adatom charge,  $e$ , is one for Na. Figure 5 shows  $OCV$  via the number of Na atoms adsorbed on GOF. The system exhibits a positive open-circuit voltage (OCV) for adsorbed Na atoms up to 21, with an average OCV of 1.3 V. The  $OCV$  is below 1.5 V which is the ideal voltage range for Na-anode material [9, 40] as well as sheets such as twin graphene and  $\text{T}_{4,4,4}$ -graphyne. The  $OCV$  displays a negative value when the

22th Na atom is absorbed. This demonstrates that GOF has a specific capacity of 947 mAh/g in the form of  $\text{Na}_{21}\text{C}_{36}$ .

For secondary ion battery electrode materials, the electronic character is crucial. Thus, investigations are conducted into the electronic band structure as well as the density of states (DOS) of GOF with and without Na atoms. The energy band gap and zero DOS at the Fermi

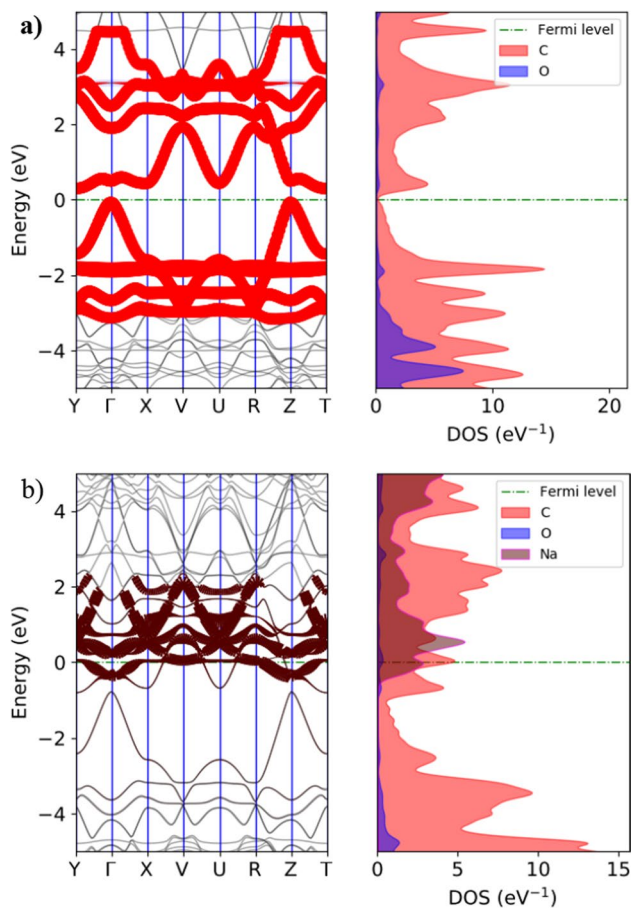


**Fig. 6** Electronic band structures and DOS of **a** GOF and **b**  $\text{Na}_4\text{C}_{36}$ . (The Fermi level is at 0 eV)

level (Fig. 6a) indicate that GOF is a semiconductor material. A small indirect band gap of 0.1 eV is seen at the  $\Gamma$  and M points. The outcome is largely consistent with an earlier study [27]. It is found that GOF becomes metal after Na adsorption. For instance, the electronic band structure and DOS of  $\text{Na}_4\text{C}_{36}$  are plotted in Fig. 6b. Due to the electronic states that cross the Fermi energy level and the non-zero DOS there,  $\text{Na}_4\text{C}_{36}$  exhibits metallic behavior. With an increase in the number of adsorbed Na ions, the band overlapping increases and the band gap disappears. Thus, GOFs have the potential to be used as a superior anode in Na-ion based batteries, as evidenced by the transition in characteristics from semiconductor to metal. The electronic band structure and DOS of the systems are also calculated under the condition of spin-polarization. The results reveal an absence of spin splitting, indicating the non-magnetic nature of the systems.

## 4 Conclusion

DFT calculations were used to study the adsorption of Na ions in GOF materials. The study investigated the most stable configuration and maximum storage capacity of GOF. The energy barrier, adsorption energy, maximum storage capacity, and open-circuit voltage were calculated to estimate the practical application of this material as an anode in Na-ion batteries. The adsorption energy falls within the ideal range for practical Na storage. AIMD simulations demonstrate that the systems exhibit acceptable thermal stability at room temperature. The low Na diffusion barrier confirms the proper mobility of Na atoms in GOF. The material exhibits high capacity and low open-circuit voltage. Additionally, a transition from semiconductor to metal was detected, which is beneficial for the material's energy storage application. Therefore, GOFs could be useful candidates for anode materials in Na-ion batteries.

**Author contributions** F.P. performed the computations and wrote the first draft of the manuscript. R.M., S.I. V, and H.R. S. completed the simulations, discussed the results, and contributed to the final manuscript.

**Data availability** Data sharing is not applicable as no new data were generated during this study.

## Declarations

**Conflict of interest** The authors declare no conflicts of interest.

## References

1. J.B. Goodenough, K.S. Park, The Li-ion rechargeable battery: a perspective. *J. Am. Chem. Soc.* **135**, 1167–1176 (2013). [https://doi.org/10.1021/JA3091438/ASSET/IMAGES/MEDIUM/JA-2012-091438\\_0009.GIF](https://doi.org/10.1021/JA3091438/ASSET/IMAGES/MEDIUM/JA-2012-091438_0009.GIF)
2. N.A. Kaskhedikar, J. Maier, Lithium storage in carbon nanostructures. *Adv. Mater.* **21**, 2664–2680 (2009). <https://doi.org/10.1002/ADMA.200901079>
3. T. Insinna, E.N. Basse, K. Märker, A. Collauto, A.L. Barra, C.P. Grey, Graphite anodes for Li-Ion batteries: an electron paramagnetic resonance investigation. *Chem. Mater.* **35**, 5497–5511 (2023). [https://doi.org/10.1021/ACS.CHEMMATER.3C00860/ASSET/IMAGES/LARGE/CM3C00860\\_0008.JPEG](https://doi.org/10.1021/ACS.CHEMMATER.3C00860/ASSET/IMAGES/LARGE/CM3C00860_0008.JPEG)
4. K. Sawai, Y. Iwakoshi, T. Ohzuku, Carbon materials for lithium-ion (shuttlecock) cells. *Solid State Ion.* **69**, 273–283 (1994). [https://doi.org/10.1016/0167-2738\(94\)90416-2](https://doi.org/10.1016/0167-2738(94)90416-2)
5. E.J. Yoo, J. Kim, E. Hosono, H.S. Zhou, T. Kudo, I. Honma, Large reversible Li storage of graphene nanosheet families for use in rechargeable lithium ion batteries. *Nano Lett.* **8**, 2277–2282 (2008). [https://doi.org/10.1021/NL800957B/SUPPL\\_FILE/NL800957B-FILE003.PDF](https://doi.org/10.1021/NL800957B/SUPPL_FILE/NL800957B-FILE003.PDF)
6. D. Sui, L. Si, C. Li, Y. Yang, Y. Zhang, W. Yan, A comprehensive review of graphene-based anode materials for lithium-ion

- capacitors. *Chemistry* **3**, 1215–1246 (2021). <https://doi.org/10.3390/CHEMISTRY3040089>
7. X. Zhang, L. Jin, X. Dai, G. Chen, G. Liu, A record-high ion storage capacity of T-graphene as two-dimensional anode material for Li-ion and Na-ion batteries. *Appl. Surf. Sci.* **527**, 146849 (2020). <https://doi.org/10.1016/J.APSUSC.2020.146849>
  8. H. Lee, B. Jang, J. Koo, M. Park, H. Lee, J. Nam, Y. Kwon, Graphdiyne as a high-capacity lithium ion battery anode material. *Appl. Phys. Lett.* **103**, 263904 (2013). <https://doi.org/10.1063/1.4850236>
  9. H. Dua, J. Deb, D. Paul, U. Sarkar, Twin-graphene as a Promising Anode Material for Na-Ion Rechargeable Batteries. *ACS Appl Nano Mater.* **4**, 4912–4918 (2021). [https://doi.org/10.1021/ACSANM.1C00460/SUPPL\\_FILE/AN1C00460\\_SI\\_001.PDF](https://doi.org/10.1021/ACSANM.1C00460/SUPPL_FILE/AN1C00460_SI_001.PDF)
  10. H.J. Hwang, J. Koo, M. Park, N. Park, Y. Kwon, H. Lee, Multilayer graphynes for lithium ion battery anode. *J. Phys. Chem. C* **117**, 6919–6923 (2013). [https://doi.org/10.1021/JP3105198/ASSET/IMAGES/MEDIUM/JP-2012-105198\\_0005.GIF](https://doi.org/10.1021/JP3105198/ASSET/IMAGES/MEDIUM/JP-2012-105198_0005.GIF)
  11. C. Vaalma, D. Buchholz, M. Weil, S. Passerini, A cost and resource analysis of sodium-ion batteries. *Nature Reviews Materials* **2018** 3:4. 3 (2018) 1–11. <https://doi.org/10.1038/natrevmats.2018.13>.
  12. M. Binder, M. Mandl, S. Zaubitzer, M. Wohlfahrt-Mehrens, S. Passerini, O. Böse, M.A. Danzer, M. Marinaro, Cover feature: sodium cyclopentadienide as a new type of electrolyte for sodium batteries (*ChemElectroChem* 2/2021). *ChemElectroChem* **8**, 272–272 (2021). <https://doi.org/10.1002/CELC.202001559>
  13. E. Goikolea, V. Palomares, S. Wang, I.R. de Larramendi, X. Guo, G. Wang, T. Rojo, Na-Ion Batteries—Approaching Old and New Challenges. *Adv. Energy Mater.* **10**, 2002055 (2020). <https://doi.org/10.1002/AENM.202002055>
  14. Y. Cao, L. Xiao, M.L. Sushko, W. Wang, B. Schwenzer, J. Xiao, Z. Nie, L.V. Saraf, Z. Yang, J. Liu, Sodium ion insertion in hollow carbon nanowires for battery applications. *Nano Lett.* **12**, 3783–3787 (2012). <https://doi.org/10.1021/NL3016957>
  15. W. Zhang, F. Zhang, F. Ming, H.N. Alshareef, Sodium-ion battery anodes: status and future trends. *EnergyChem.* **1**, 100012 (2019). <https://doi.org/10.1016/J.ENCHEM.2019.100012>
  16. Z. Xu, X. Lv, J. Li, J. Chen, Q. Liu, A promising anode material for sodium-ion battery with high capacity and high diffusion ability: graphyne and graphdiyne. *RSC Adv.* **6**, 25594–25600 (2016). <https://doi.org/10.1039/C6RA01870J>
  17. A.H. Farokh Niaei, T. Hussain, M. Hankel, D.J. Searles, Sodium-intercalated bulk graphdiyne as an anode material for rechargeable batteries. *J Power Sources.* **343** (2017) 354–363. <https://doi.org/10.1016/J.JPOWSOUR.2017.01.027>.
  18. J. Deb, R. Ahuja, U. Sarkar, Two-Dimensional Pentagraphyne as a High-Performance Anode Material for Li/Na-Ion Rechargeable Batteries. *ACS Appl Nano Mater.* **5**, 10572–10582 (2022). [https://doi.org/10.1021/ACSANM.2C01909/SUPPL\\_FILE/AN2C01909\\_SI\\_001.PDF](https://doi.org/10.1021/ACSANM.2C01909/SUPPL_FILE/AN2C01909_SI_001.PDF)
  19. R. Majidi, A.I. Ayesh, A density functional theory study of twin T-graphene as an anode material for Na-ion-based batteries. *J. Appl. Phys.* **132**, 194301 (2022). <https://doi.org/10.1063/5.0123013>
  20. R. Majidi, A.I. Ayesh, Application of T4,4,4-graphyne for anode of Na-ion battery: first principle theoretical study. *Mol. Simul.* **49**, 1044–1050 (2023). <https://doi.org/10.1080/08927022.2023.2211170>
  21. X. Bai, N. Wu, G. Yu, T. Li, Recent Advances in Anode Materials for Sodium-Ion Batteries, *Inorganics* **2023**, Vol. 11, Page 289. 11 (2023) 289. <https://doi.org/10.3390/INORGANICS11070289>.
  22. Y. Wen, K. He, Y. Zhu, F. Han, Y. Xu, I. Matsuda, Y. Ishii, J. Cumings, C. Wang, Expanded graphite as superior anode for sodium-ion batteries. *Nature Communications* **2014** 5:1. 5 (2014) 1–10. <https://doi.org/10.1038/ncomms5033>.
  23. S.U.D. Shamim, M.K. Hossain, S.M. Hasan, A.A. Piya, M.S. Rahman, M.A. Hossain, F. Ahmed, Understanding Na-ion adsorption in nitrogen doped graphene oxide anode for rechargeable sodium ion batteries. *Appl. Surf. Sci.* **579**, 152147 (2022). <https://doi.org/10.1016/J.APSUSC.2021.152147>
  24. S. Gadipelli, Z.X. Guo, Graphene-based materials: Synthesis and gas sorption, storage and separation. *Prog. Mater. Sci.* **69**, 1–60 (2015). <https://doi.org/10.1016/J.PMATSCI.2014.10.004>
  25. G. Srinivas, J.W. Burress, J. Ford, T. Yildirim, Porous graphene oxide frameworks: Synthesis and gas sorption properties. *J. Mater. Chem.* **21**, 11323–11329 (2011). <https://doi.org/10.1039/C1JM11699A>
  26. J.W. Burress, S. Gadipelli, J. Ford, J.M. Simmons, W. Zhou, T. Yildirim, Graphene oxide framework materials: theoretical predictions and experimental results. *Angew. Chem. Int. Ed.* **49**, 8902–8904 (2010). <https://doi.org/10.1002/ANIE.201003328>
  27. P. Zhu, B.G. Sumpter, V. Meunier, Electronic, thermal, and structural properties of graphene oxide frameworks. *J. Phys. Chem. C* **117**, 8276–8281 (2013). [https://doi.org/10.1021/JP401072Z/ASSET/IMAGES/MEDIUM/JP-2013-01072Z\\_0006.GIF](https://doi.org/10.1021/JP401072Z/ASSET/IMAGES/MEDIUM/JP-2013-01072Z_0006.GIF)
  28. I. Skarmoutsos, E.N. Koukaras, E. Klontzas, A computational study on phenyldiboronic acid-pillared graphene oxide frameworks for gas storage and separation. *ACS Appl Nano Mater.* **5**, 9286–9297 (2022). [https://doi.org/10.1021/ACSANM.2C01617/ASSET/IMAGES/MEDIUM/AN2C01617\\_0011.GIF](https://doi.org/10.1021/ACSANM.2C01617/ASSET/IMAGES/MEDIUM/AN2C01617_0011.GIF)
  29. G. Mercier, A. Klechikov, M. Hedenström, D. Johnels, I.A. Baburin, G. Seifert, R. Mysyk, A.V. Talyzin, Porous graphene oxide/diboronic acid materials: structure and hydrogen sorption. *J. Phys. Chem. C* **119**, 27179–27191 (2015). [https://doi.org/10.1021/ACS.JPCC.5B06402/ASSET/IMAGES/LARGE/JP-2015-064029\\_0014.JPEG](https://doi.org/10.1021/ACS.JPCC.5B06402/ASSET/IMAGES/LARGE/JP-2015-064029_0014.JPEG)
  30. Y. Chan, J.M. Hill, Hydrogen storage inside graphene-oxide frameworks. *Nanotechnology* **22**, 305403 (2011). <https://doi.org/10.1088/0957-4484/22/30/305403>
  31. User's manual of OpenMX Ver. 3.9. (n.d.). [http://www.openmx-square.org/openmx\\_man3.9/index.html](http://www.openmx-square.org/openmx_man3.9/index.html). Accessed 5 Oct 2022
  32. J.P. Perdew, K. Burke, M. Ernzerhof, Generalized gradient approximation made simple. *Phys. Rev. Lett.* **77**, 3865–3868 (1996). <https://doi.org/10.1103/PhysRevLett.77.3865>
  33. S. Grimme, S. Ehrlich, L. Goerigk, Effect of the damping function in dispersion corrected density functional theory. *J. Comput. Chem.* **32**, 1456–1465 (2011). <https://doi.org/10.1002/jcc.21759>
  34. S. Grimme, J. Antony, S. Ehrlich, H. Krieg, A consistent and accurate ab initio parametrization of density functional dispersion correction (DFT-D) for the 94 elements H-Pu. *J. Chem. Phys.* **132**, 154104 (2010). <https://doi.org/10.1063/1.3382344>
  35. G. Henkelman, H. Jónsson, Improved tangent estimate in the nudged elastic band method for finding minimum energy paths and saddle points. *J. Chem. Phys.* **113**, 9978 (2000). <https://doi.org/10.1063/1.1323224>
  36. M. Nasrollahpour, M. Vafae, M.R. Hosseini, H. Iravani, Ab initio study of sodium diffusion and adsorption on boron-doped graphyne as promising anode material in sodium-ion batteries. *Phys. Chem. Chem. Phys.* **20**, 29889–29895 (2018). <https://doi.org/10.1039/C8CP04088E>
  37. R. Majidi, A. Ramazani, T. Rabczuk, Electronic properties of transition metal embedded twin T-graphene: A density functional theory study. *Physica E Low Dimens Syst Nanostruct.* **133**, 114806 (2021). <https://doi.org/10.1016/J.PHYSE.2021.114806>
  38. J. Hu, Y. Liu, N. Liu, J. Li, C. Ouyang, Theoretical prediction of T-graphene as a promising alkali-ion battery anode offering ultrahigh capacity. *Phys. Chem. Chem. Phys.* **22**, 3281–3289 (2020). <https://doi.org/10.1039/C9CP06099E>
  39. C. Kittel, P. McEuen, Introduction to solid state physics, (n.d.) 692. <https://www.wiley.com/en-ie/Kittel%27s+Introduction+to+>

- [Solid+State+Physics%2C+8th+Edition%2C+Global+Edition-p-9781119454168](#) (accessed December 1, 2023).
40. T. Singh, J.R. Choudhuri, M.K. Rana,  $\alpha$ -graphyne as a promising anode material for Na-ion batteries: a first-principles study. *Nanotechnology* **34**, 045404 (2022). <https://doi.org/10.1088/1361-6528/AC9A54>

Springer Nature or its licensor (e.g. a society or other partner) holds exclusive rights to this article under a publishing agreement with the author(s) or other rightsholder(s); author self-archiving of the accepted manuscript version of this article is solely governed by the terms of such publishing agreement and applicable law.

**Publisher's Note** Springer Nature remains neutral with regard to jurisdictional claims in published maps and institutional affiliations.